Journal of Materials Chemistry C

Accepted Manuscript

This article can be cited before page numbers have been issued, to do this please use: S. Jeong, Y. Lee, J. K. Kim, D. Jang and J. Hong, *J. Mater. Chem. C*, 2018, DOI: 10.1039/C8TC02590H.

Volume 4 | Number 1 | 7 January 2016 | Pages 1–224

Journal of Materials Chemistry C

Materials for optical, magnetic and electronic devices

www.rsc.org/MaterialsC

ISSN 2050-7526

ROYAL SOCIETY OF CHEMISTRY

PAPER
Nguyễn T. K. Thanh, Xiaodi Su *et al.*
Fine-tuning of gold nanorod dimensions and plasmonic properties using the Hofmeister effects

175 YEARS

View Article Online
DOI: 10.1039/C8TC02590H

Journal of Materials Chemistry C

PAPER

Received 00th January 20xx,
Accepted 00th January 20xx

DOI: 10.1039/x0xx00000x

www.rsc.org/

Non-doped Thermally Activated Delayed Fluorescent Organic Light-emitting Diodes Using an Intra- and Intermolecular Exciplex System with a Meta-linked Acridine-Triazine Conjugate

Seongjin Jeong, Youngnam Lee, Joon Ki Kim, Du-Jeon Jang and Jong-In Hong*

We report OLEDs utilizing non-doped TADF emitters, 10-(3-(4,6-diphenyl-1,3,5-triazin-2-yl)phenyl)-9,9-dimethyl-9,10-dihydroacridine (AmT) and 10-(3'-(4,6-diphenyl-1,3,5-triazin-2-yl)-[1,1'-biphenyl]-3-yl)-9,9-dimethyl-9,10-dihydroacridine (AmmT). These two emitters are composed of electron donor (acridine) and acceptor (triphenyltriazine) moieties, which are connected at the meta positions so that intra- and intermolecular charge transfer (CT) states can be induced through exciplex-like interactions between the same emitters. A neat film of AmmT forms intermolecular CT state-induced exciplexes more favorably than AmT because of the packing benefits and relatively shorter radiative lifetime of AmmT. Electroluminescent devices using AmmT as an emitter exhibit an external quantum efficiency (EQE) over 18%, which is much better than the EQE value for devices using AmT. This is the first example of a non-doped TADF system using a single molecule-based exciplex as a dominant exciton source.

1. Introduction

Since the 1987 report by Tang and Vanslyke, organic light-emitting diodes (OLEDs)[1] have continued to draw attention because of their many possible applications in future displays, from smart phones to large flat panel displays.[2] The vast majority of previous fluorescent emitting layers (EML) of OLED devices were constructed using a host-dopant system (doping system).[3,4,5] Controlling intermolecular interactions through the doping system made it possible to achieve high-efficiency luminescence characteristics by preventing concentration quenching and controlling the color purity. However, the device performance of the doping system would seriously deteriorate during operation because of inherent phase separation.[4] In addition, a scrupulous design of the appropriate host is required based on the energy gap and charge-transporting characteristics of the dopant material. Therefore, developing non-doped (or host-free) emitters is desirable because the non-doped system has a simple device structure that employs only a single emitting material without using a complicated host-dopant co-deposition process.[6,7]

Recently, there have been continuous efforts to overcome the limitations of fluorescence-based OLED devices by harvesting long-lived triplet excitons through thermally activated delayed fluorescence (TADF) utilizing additionally generated singlet excitons without using heavy atoms.[8,9] This approach can provide 100% internal quantum efficiency (IQE) because the triplet can be converted to a singlet because of the small energy difference between the singlet and triplet states (ΔE_{ST}), which leads to efficient reverse intersystem crossing (RISC). In TADF molecules, donor and acceptor moieties have limited electronic interactions, by their orthogonal arrangement as a result of steric hindrance, or by increasing the distance between them. Therefore, TADF molecules have small ΔE_{ST} and emit light by charge transfer (CT) processes with a high IQE.[10,11] This makes it possible to overcome the efficiency problems of fluorescent materials.

However, TADF molecules can easily aggregate through π–π interactions that arise from their innate hydrophobicity and rigid planar structures and lead to aggregation-caused quenching (ACQ) and exciton concentration quenching in the solid state.[11-13] These phenomena fatally weaken the OLEDs using solid-state emission. To overcome these problems, a doping system was introduced into the EML of TADF OLED devices, despite the aforementioned drawbacks.[14] An alternative method to avoid ACQ is to use aggregation-induced emission (AIE).[15,16] An external quantum efficiency (EQE) of approximately 10% was obtained in an OLED device using non-doped EML materials that caused AIE and TADF.[17] However, there are a few reports of highly efficient OLED devices using AIE-TADF systems.

Department of Chemistry, College of Natural Sciences, Seoul National University, Seoul 151-747, Republic of Korea, E-mail: jihong@snu.ac.kr.

† Electronic Supplementary Information (ESI) available: [details of any supplementary information available should be included here]. See DOI: 10.1039/x0xx00000x

View Article Online
DOI: 10.1039/C8TC02590H

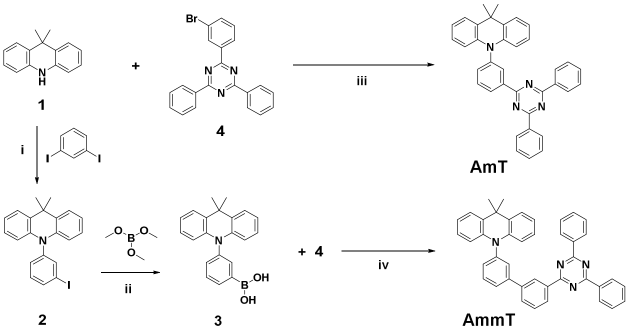

(i) Cu powder, K_2CO_3, o-dichlorobenzene, reflux, under N_2; (ii) n-BuLi, THF, -78°C, under N_2;
(iii) $Pd(OAc)_2$, KO^tBu, $P^tBu_3HBF_4$, toluene, reflux, under N_2; (iv) $Pd(PPh_3)_4$, K_2CO_3 (2M aq), THF/H_2O, reflux

Scheme 1. Synthetic routes of AmT and AmmT.

Since the report by Kim et al. in 2012, there have been many reports on TADFs using intermolecular CT complexes based on two different materials (exciplex system).[18,19] One can easily achieve appropriate charge balance and reduce the quenching process by lowering the charge carrier and exciton density in the EML using exciplex systems.[20,21] Above all, exciplex systems should provide a small ΔE_{ST}. However, exciplex systems require careful consideration of the highest occupied molecular orbital (HOMO) and lowest unoccupied molecular orbital (LUMO) energies of the donor and acceptor, respectively. In addition, it is important to have the optimum ratio of donor and acceptor materials when fabricating the device, because slight deviation in the optimum donor/acceptor molar ratio can cause a significant decrease in the device performance by breaking the charge carrier balance of the device.[22,23] Therefore, we developed a non-doped TADF system based on a single molecule exciplex with the advantages of the exciplex system and the non-doped TADF.

In this study, we designed two emitting materials that have delayed fluorescence (DF) character by their intra- and intermolecular interactions; 10-(3-(4,6-diphenyl-1,3,5-triazin-2-yl)phenyl)-9,9-dimethyl-9,10-dihydroacridine (AmT) and 10-(3'-(4,6-diphenyl-1,3,5-triazin-2-yl)-[1,1'-biphenyl]-3-yl)-9,9-dimethyl-9,10-dihydroacridine (AmmT). AmT and AmmT consist of an acridine (Ac) donor and a triphenyltriazine (TRZ) acceptor, and have phenyl and biphenyl linkers that are connected to the donor and the diphenyltriazine moiety of the acceptor, respectively, through a meta linkage. Calculated structures of AmT and AmmT show that the electron distributions of the HOMO and LUMO are almost separated, providing small exchange energies and almost the same singlet and triplet energy levels. Because of the meta-positioned phenyl and biphenyl moieties, ICT-induced absorption bands of AmT and AmmT were not observed, and the resulting low oscillator strength should lead to poor luminescence. However, a strong emission with a large Stokes shift was observed in the neat film of AmT or AmmT; it originated from the intermolecular CT state (like exciplex) corresponding to the difference between the HOMO of the emitter donor moiety and the LUMO of the emitter acceptor moiety. This phenomenon results from the more favorable formation of an intermolecular exciplex in the neat film than in solution because of the reduced intermolecular distances in the neat film. In addition, AmT and AmmT show DF. Photophysical and single crystal X-ray structural analyses confirmed that intermolecular CT-induced DF can occur more effectively in AmmT because AmmT molecules are more uniformly and tightly packed in the neat film than AmT. OLEDs using AmmT as an emitter without a host showed an EQE above 18%, which is better than the EQE value of AmT-based OLEDs, because of the more efficient formation of intermolecular exciplexes of AmmT. This is the first example of TADF molecules utilizing intermolecular CT excitons (exciplex) between donor-acceptor-type emitter molecules of a single species.

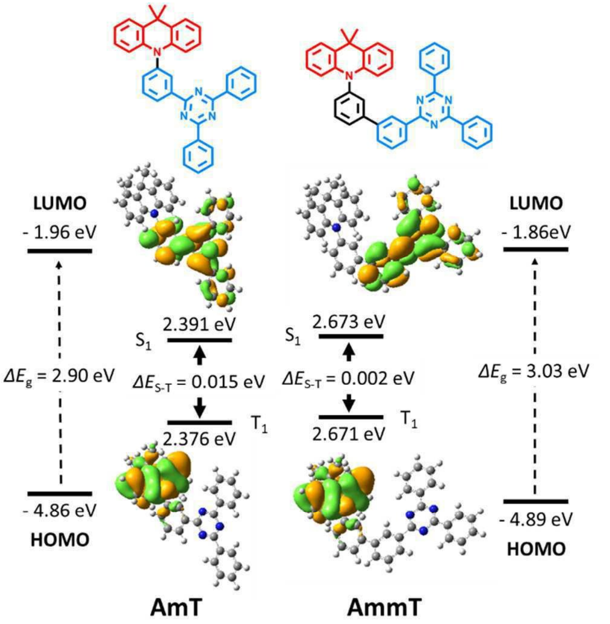

Fig. 1. Molecular structures, HOMO and LUMO distributions and calculated singlet and triplet energy levels from time-dependent density functional theory calculations at the B3LYP/6-31G(d) level.

2. Results and discussion

2.1 Synthesis of AmT and AmmT

The synthetic routes of AmT and AmmT are illustrated in Scheme 1. 9,9-Dimethyl-9,10-dihydroacridine (Ac, 1) and 2-(3-bromophenyl)-4,6-diphenyl-1,3,5-triazine (4) were synthesized according to previous methods.[24,25] 10-(3-Iodophenyl)-9,9-dimethyl-9,10-dihydroacridine (2) was obtained using the Ullmann cross coupling reaction between compound 1 and 1,3-diiodobenzene. (3-(9,9-dimethylacridin-10(9*H*)-yl)phenyl)-boronic acid (3) was synthesized by reacting compound 2 with trimethyl borate at -78 □. AmT and AmmT were prepared by Buchwald cross coupling between compounds 1 and 4 and by Suzuki cross coupling using compounds 3 and 4, respectively. AmT and AmmT were characterized by ^1H NMR, ^{13}C NMR, and low- and high-resolution mass spectrometry. These two compounds were purified further by train sublimation (twice) under a reduced pressure (<10^{-4} Torr).

View Article Online
DOI: 10.1039/C8TC02590H

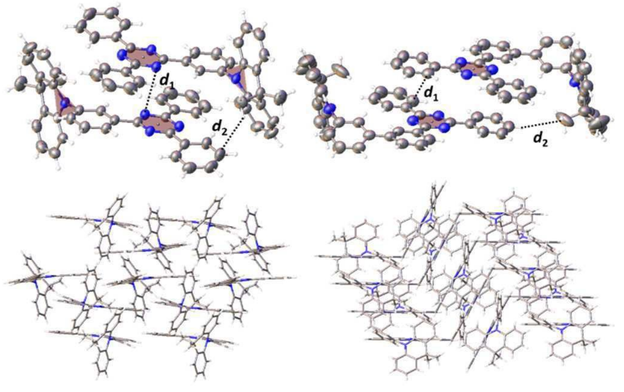

Fig. 2. Packing patterns of AmT (left, d1 = 3.455 Å, d2 = 3.137 Å) and AmmT (right, d1 = 3.494 Å, d2 = 3.122 Å).

2.2 DFT Calculations and Crystallography

Fig. 1 depicts the molecular structures and theoretical simulation of AmT and AmmT. The optimized geometries and electron density distributions of the frontier molecular orbitals were investigated using time-dependent density functional theory calculations at the B3LYP/6-31G(d) level using Gaussian '09. The HOMOs of AmT and AmmT are located on the Ac donors, whereas the LUMOs are distributed over the TRZ acceptors. The HOMO of AmT is extended slightly to the neighboring phenyl of the TRZ acceptor while its LUMO is extended over TRZ. There is a small orbital overlap between the HOMO and LUMO of AmT in the connecting phenyl moiety of TRZ, as shown in Fig. 1. In contrast, the calculated structure of AmmT shows totally separated electron distributions of the HOMO and LUMO because of an additional meta-linked phenylene moiety. Thus, AmT shows a small ΔE_{ST} value of 0.015 eV, whereas that of AmmT is even lower (0.002 eV).

Single crystal X-ray diffraction analysis of AmT and AmmT (grown from a dichloromethane-cyclopentane mixed solvent) reveals that the torsion angles between the Ac donor and the phenyl linker of AmT and AmmT are 79° and 81°, respectively. In addition, the dihedral angle between the two benzene rings of the biphenyl group in AmmT is 31°, providing additional twisting (Fig. S1).[26] Details of the single-crystal structures of AmT and AmmT are given in Table S1.

Fig. 2 shows the packing patterns of AmT and AmmT in single crystals. For AmT, alternating pairs of adjacent TRZ moieties are partially stacked with distances of 3.455-3.512 Å. However, all pairs of adjacent planar TRZ moieties in AmmT are parallel, and their π-surfaces partially overlap with alternating distances of 3.452 and 3.494 Å; these properties would be beneficial for charge transport. Closely packed AmmT molecules in the crystal structure are expected to provide a more efficient environment for intermolecular interactions, thereby increasing the efficiency of exciplex (exciton) formation.

2.3 Photophysical properties in solution

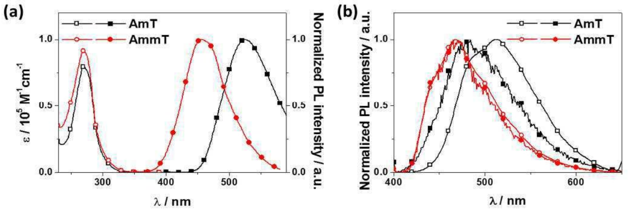

Fig. 3. (a) UV-Vis (10 μM in dichloromethane) and PL spectra (10 μM in toluene) of AmT and AmmT, and (b) low temperature PL spectra (77 K, 10 μM in 2-methyltetrahydrofuran); open symbol with line: low temperature fluorescence, closed symbol with line: phosphorescence

The photophyscial properties of AmT and AmmT were analyzed using ultraviolet-visible (UV-Vis) and photoluminescence (PL) spectroscopies, and transient PL decay measurements. At room temperature (300 K), each compound shows almost the same UV-Vis absorbance around 270 nm, which is attributed to the π-π* absorption band from the Ac donor and the TRZ acceptor in the dichloromethane solution (Fig. 3(a)).[27,28] Both materials do not exhibit any ICT-induced absorption bands above 300 nm because of the limited electronic interactions by the meta-positioned donor and acceptor moieties. However, the two compounds exhibit dim, broad emission with a large Stokes shift (187 nm and 256 nm for AmT and AmmT, respectively) in toluene. The triplet energy levels of AmT and AmmT were estimated by the emission onset of the PL spectra at 77 K to be 2.94 and 2.97 eV, respectively (Fig. 3(b)). The low temperature fluorescence and phosphorescence (20 ms time delay) spectra of AmT show λ_{max} values at 514 and 484 nm, respectively. AmmT shows the same low temperature fluorescence and phosphorescence spectra at 468 nm. The structureless fluorescence and phosphorescence emission spectra of AmT and AmmT at low temperature indicate that their emissions are dominated by the CT state, which means that the T_1 states of AmT and AmmT originate from the ^{3}CT state. We examined the PL solvatochromic shift of AmT and AmmT using various solvents at room temperature (Fig. S2). Both materials show that the PL spectra are red-shifted, and the PL intensities decrease as the dielectric constant of the solvents increases. This indicates that their emissive S_1 states are dependent on the dielectric constant of the solvent.

2.4 Intra- and intermolecular exciplex formation

Because of the extremely low luminescence of the dilute CH_2Cl_2 solution (10 μM) of AmT and AmmT at room temperature, we wanted to investigate the luminescence characteristics according to the state of aggregation in tetrahydrofuran/water mixtures (Fig. S3).[29] Particularly, the PL intensities of AmmT are almost similar when the water fraction (f_w) is less than 70%. When the f_w is larger than 70%, the PL intensities increase, indicating AIE-like behavior.

As shown in Fig. 3(a), AmT and AmmT do not show ICT absorption bands. However, the large solvatochromic shift observed in AmT and AmmT is likely due to CT from the Ac donor to the TRZ acceptor. This was supported by additional photophysical experiments using Ac and 9,9-dimethyl-10-phenyl-9,10-dihydroacridine (PhAc) as the donors of AmT and

View Article Online
DOI: 10.1039/C8TC02590H

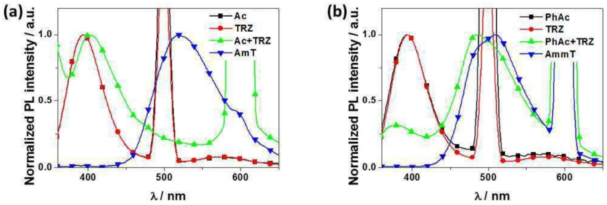

Fig. 4. PL spectra of spin-coated films of Ac, 9,9-dimethyl-10-phenyl-9,10-dihydroacridine (PhAc), TRZ, and (a) a mixture of Ac and TRZ (1:1 molar ratio) and a neat film of AmT, and (b) a mixture of PhAc and TRZ (1:1 molar ratio) and a neat film of AmmT. PL peaks at 500 nm are the 2nd harmonic wavelength of excitation about Ac, PhAc and TRZ. PL peaks at 600 nm are the 2nd harmonic wavelength of excitation about AmT and AmmT.

AmmT, respectively, and TRZ as the acceptor. Fig. 4 shows PL spectra of Ac:TRZ (1:1 molar ratio, film) and PhAc:TRZ (1:1 molar ratio, film) along with those of Ac, PhAc, and TRZ films. The PL spectra of Ac, PhAc, and TRZ are almost the same with a maximum wavelength of 400 nm. The PL spectrum of the 50 mol% Ac:TRZ film is similar to that of the Ac or TRZ film; however, that of the 50 mol% PhAc:TRZ film is significantly red-shifted compared to that of the PhAc or TRZ film. In particular, the PL spectrum of the 50 mol% PhAc:TRZ film is similar to that of the AmmT neat film. Cyclic voltammetry (CV) measurements revealed that the HOMO energy levels of Ac and PhAc are 5.12 and 5.30 eV, respectively, and the LUMO energy level of TRZ is 2.48 eV (Fig. S4). These results indicate that the emission of AmT results from the intramolecular exciplex-like formation between the HOMO of Ac and the LUMO of TRZ, and the emission of AmmT comes mostly from the intermolecular exciplex-like system between the HOMO of PhAc and the LUMO of TRZ.

2.5 Photophysical properties in films

The photophysical properties of AmT and AmmT in neat and doped films (20 wt% in bis[2-(diphenylphosphino)phenyl] ether oxide (DPEPO)) were also investigated at room temperature (Fig. 5). The λ_{max} absorption peaks of AmT are 276 and 283 nm in the neat and doped films, respectively, and those of AmmT appear at 283 and 284 nm, respectively. The estimated emission onset of the PL spectra of AmT in both the neat and doped films was 456 nm, which corresponds to the optical bandgap of 2.72 eV. In contrast, the measured emission onset values of the PL spectra of AmmT in the neat and doped films were 443 and 427 nm, respectively, which correspond to optical bandgaps of 2.80 and 2.91 eV, respectively. The LUMO energy levels of AmT and AmmT in the neat film are 2.81 and 2.68 eV, respectively, which were calculated from the optical bandgap and the HOMO energy levels of 5.53 and 5.48 eV for AmT and AmmT, respectively, estimated from the CV in a dichloromethane solution (Fig. S4(a)). The LUMO energy levels were obtained from CV measurements (Fig. S4(b)). The PL λ_{max} values of AmT in the neat and doped films are 519 and 522 nm, respectively. The PL λ_{max} values of AmmT in the neat and doped films are 509 and 480 nm, respectively. The PL quantum yields of the neat and doped films (measured using integrating spheres) are 0.52 and 0.27 (AmT), respectively, and 0.69 and 0.20 (AmmT), respectively. The higher PL quantum yields of AmT and AmmT in the neat film than those in the doped film indicate that the CT exciton formed in the neat film is better than that of the doped film because of the decreased intermolecular distances in the neat film. This suggests that a crucial factor that affects the luminance of AmT and AmmT is the formation of CT excitons by intermolecular interactions, not the AIE phenomenon by restricting the intramolecular rotation.[30] The higher PL quantum yield of AmT in the doped film than that of AmmT in the doped film indicates that the intramolecular exciplex formation of AmT is better than that of AmmT. However, the PL quantum yield of AmmT in the neat film is much higher than that of AmT in the neat film because formation of an intermolecular exciplex is more favorable for AmmT than for AmT.

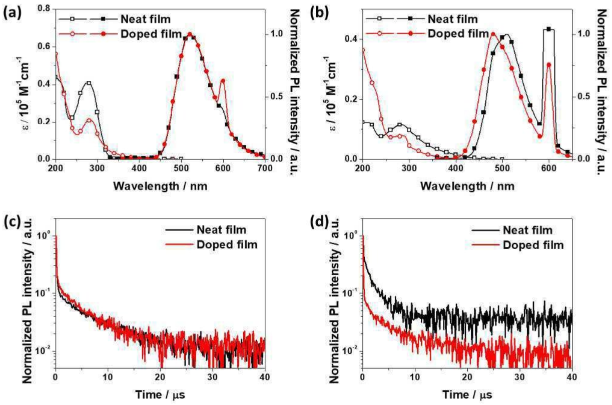

Fig. 5. UV and PL spectra of neat and doped (20 wt% in a bis[2-(diphenylphosphino)phenyl] ether oxide (DPEPO) host) films of (a) AmT and (b) AmmT. PL peaks at 600 nm are the 2nd harmonic wavelength of excitation. Transient PL decay spectra of doped (20% in DPEPO) and neat films at 300 K of (c) AmT and (d) AmmT.

Fig. 5 (c) and (d) also depict the transient PL decay curves of the neat and doped films of AmT and AmmT at room temperature, and show double-exponential decay profiles, confirming the existence of the DF. The prompt component is assigned to an intra- and intermolecular exciplex, and the delayed component is attributed to (identical) DF occurring via the RISC process. The neat and doped films of AmT have prompt fluorescence decay times (τ_{PF}) of 93 and 79 ns, respectively, and the delayed fluorescence decay time (τ_{DF}) of 5.80 and 4.32 μs, respectively. The neat and doped films of AmmT exhibit τ_{PF} values of 59 and 72 ns, respectively, and τ_{DF} values of 1.76 and 4.01 μs, respectively. The τ_{PF} and τ_{DF} values of the neat film of AmmT are smaller than those of the doped film of AmmT, suggesting a more efficient radiative decay in the neat film than in the doped film. The PL quantum yields of AmmT contributed by a prompt component (Φ_{PF}) and delayed component (Φ_{DF}) were estimated from the decay lifetime and its amplitude (Table S2) as 0.16 and 0.53 in the neat film, respectively, while the values of Φ_{PF} and Φ_{DF} of AmmT are 0.04 and 0.16, respectively, in the doped film. However, the values of Φ_{PF} and Φ_{DF} of the AmT neat film are 0.16 and 0.36, respectively, and those of the AmT doped film are 0.08 and 0.19, respectively. Regardless of prompt or delayed fluorescence, the PL quantum yields of the AmmT neat film are 3 to 4 times higher than those of the AmmT doped film because of the decreased intermolecular distances, whereas the AmT

View Article Online
DOI: 10.1039/C8TC02590H

neat film showed PL quantum yields that were twice the value of those for the doped film of AmT.

2.6 TADF properties

We investigated the temperature dependence of the transient PL decay of AmT and AmmT measured from 78 to 300 K. The DF increases with temperature, indicating that AmT and AmmT exhibit strong TADF characters in both the neat and doped films (Fig. S5). The RISC rate values (k_{RISC}) were estimated using the equations provided in the supplementary notes, and the calculated ΔE_{ST} values in the neat and doped films were 33.6 and 34.4 meV for AmT, and 56.5 and 31.7 meV for AmmT, respectively, from the Arrhenius plots of k_{RISC} between 125 and 250 K, as shown in Fig. S6. The values of k_{RISC} for the doped films of AmmT did not show a clear temperature dependence. This is because formation of the intermolecular (exciplex) CT excitons for the doped film of AmmT is less efficient than that of the neat film (because of the relatively long distances between AmmT molecules in the doped film).

2.7 Device performances

Non-doped devices were fabricated using AmT and AmmT as emitters in the EML with the following device configuration: glass substrate/indium tin oxide/N,N'-di(1-naphthyl)-N,N'-diphenyl-(1,1-biphenyl)-4,4'-diamine (NPB) (30 nm)/4,4'-cyclohexylidenebis[N,N-bis(4-methylphenyl)benzenamine] (TAPC) (30 nm)/AmT or AmmT (20 nm)/DPEPO (10 nm)/2,2',2''-(1,3,5-benzinetriyl)-tris(1-phenyl-1-*H*-benzimidazole) (TPBI) (40 nm)/LiF (1 nm)/Al (100 nm). The following components were deposited on the substrate in sequential order: NPB and TAPC as hole transporting layers, DPEPO with a deep HOMO energy level and high triplet energy (3.1 eV) as a hole blocking and an exciton confinement layer, TPBI as an electron transporting layer, an LiF as an electron injection layer, and Al cathode. Two different OLEDs were fabricated, and the performance of each device was evaluated (Table S3). Fig. 6(a) shows the current density–voltage characteristics of each device with AmT and AmmT. The current density of the device with AmT is higher than that of the device with AmmT, whereas the luminance values and turn-on voltage of each device are similar at the same driving voltage as shown in Fig. 6(b). Although AmmT-based devices show worse current density-voltage characteristics than AmT-based devices, the similar luminance values and turn-on voltages of the two devices indicate that AmmT-based devices generate intermolecular exciplexes more efficiently because of the high packing density of AmmT molecules in the non-doped environment; thus, AmmT-based devices produce light emission better than AmT-based devices. Quantum efficiency–luminance characteristics of two devices were plotted in Fig. 6(c). AmmT-based devices show a maximum EQE of 18.66%, which is much higher than that of AmT based-devices (5.30%).

To understand the reasons for high efficiency of non-doped devices, we fabricated additional devices using 20 wt% AmT and AmmT doped into DPEPO in the EML (Fig. S7). AmT- and AmmT-doped devices show maximum EQEs of 4.19% and 3.28%, respectively, supporting that the formation of an intermolecular CT exciton is a major contributor to the high efficiency of non-doped devices. The EQE of AmmT-based non-doped devices is about 3.5 times higher than that of AmT-based devices, and about 3.6-5.4 times higher than the theoretical maximum EQE of approximately 3.45% to 5.18% (out-coupling efficiency = 0.2−0.3), assuming that the EL quantum efficiency is the same as the PL quantum efficiency of 0.69. Fig. 6(d) shows normalized EL spectra obtained using non-doped devices. Inherent EL emission λ_{max} values of the AmT- and AmmT-based devices were observed at 524 and 504 nm, respectively, without any other emission from the adjacent layers.

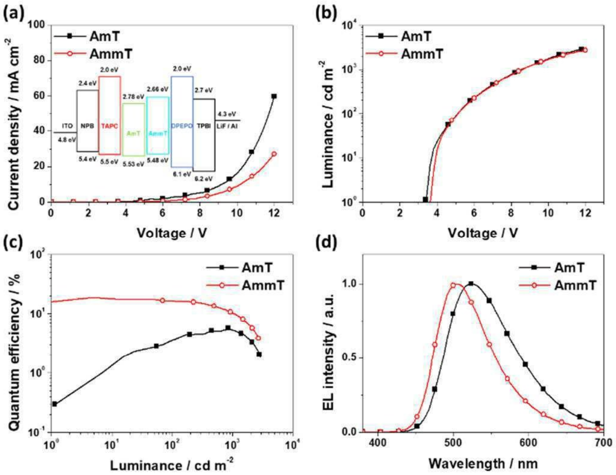

Fig. 6. Electroluminescent (EL) characteristics of AmT- and AmmT-based devices using a non-doped system. (a) Current density-voltage characteristics (inset: energy level diagram of each device), (b) luminance-voltage characteristics (inset: device structure), (c) quantum efficiency-luminance characteristics, and (d) EL spectra.

Donor-acceptor-type TADF materials do not generally emit fluorescence by a Förster resonance energy transfer (FRET) mechanism because they have a small overlap between absorption and emission (large Stokes shift).[31] Therefore, the effect of concentration quenching by FRET (of singlet excitons in the luminescence process) of AmT and AmmT is also negligible. In contrast, concentration quenching by electron-exchange interactions (for triplet excitons) is partially considered. Recently, Yasuda and co-workers reported that concentration quenching of TADF molecules was dominated by electron-exchange interactions for triplet excitons using the Dexter energy-transfer (DET) model.[32] The maximum EQE of 18.66% in the AmmT-based device suggests that the exciton quenching in the neat film of AmmT is mainly caused by the DET process, but it is insignificant compared to the CT excitons generated by intermolecular interactions, as shown by the experimental results of the neat and doped films.

3. Conclusions

In conclusion, we developed TADF molecules (AmT and AmmT) for highly efficient non-doped OLEDs utilizing intra- and intermolecular CT excitons, which are composed of meta-

View Article Online
DOI: 10.1039/C8TC02590H

linked Ac donor and TRZ acceptor molecules. Intermolecular CT excitons of AmT and AmmT are generated more favorably under non-doped conditions than in solution or under doped conditions because of their spatial proximity. This means that efficient formation of CT excitons results from intermolecular interactions, rather than by AIE. AmT and AmmT are the first TADF molecules based on intermolecular CT exciplexes between donor-acceptor-type emitter molecules of a single species. While AmT shows more efficient intramolecular CT exciton formation than AmmT, the neat film of AmmT forms an intermolecular CT state-induced exciplex better than AmT because of the packing benefits and relatively shorter radiative lifetime of AmmT. As a result, EL devices that use AmmT as an emitter without a host exhibit an EQE over 18%. A single molecule exciplex-based TADF system using intra- and intermolecular CT excitons could be useful for developing high efficiency non-doped OLEDs.

Conflicts of interest

There are no conflicts to declare.

Acknowledgements

This work was supported by the NRF grant (2018R1A2B2001293) funded by the MSIP. We thank the Samsung Display Co., Ltd. for partial financial support. Equipments for low temperature PL experiments were supported by CSOM (Prof. S. Y. Park). We are also grateful to Ms. B. Sim (Prof. J. Kim) for measurements of absolute PL quantum yields.

Notes and references

1 C. W. Tang, S. A. Vanslyke, *Appl. Phys. Lett.*, 1987, **51**, 913-915.
2 K. Müllen, U. Scherf, *Organic Light Emitting Devices: Synthesis, Properties and Applications, Wiley-VCH, Weinheim, Germany*, 2006.
3 Y. J. Pu, G. Nakata, F. Satoh, H. Sasabe, D. Yokoyama, J. Kido, *Adv. Mater.*, 2012, **24**, 1765-1770.
4 M. Zhu, C. Yang, *Chem. Soc. Rev.*, 2013, **42**, 4963-4976.
5 D. Y. Kondakov, *J. Soc. Inf. Disp.*, 2009, **17**, 137-144.
6 S. Jeong, J.-I. Hong, *Dyes and Pigments,* 2017*,* **144**, 9-16.
7 S. Jeong, M.-K. Kim, S. H. Kim, J.-I. Hong, *Org. Electron.*, 2013, **14**, 2497-2504.
8 A. Endo, K. Sato, K. Yoshimura, T. Kai, A. Kawada, H. Miyazaki, C. Adachi, *Appl. Phys. Lett.*, 2011, **98**, 083302.
9 H. Uoyama, K. Goushi, K. Shizu, H. Nomura, C. Adachi, *Nature*, 2012, **492**, 234-240.
10 M. Kim, S. K. Jeon, S. H. Hwang, J. Y. Lee, *Adv. Mater.*, 2015, **27**, 2515-2520.
11 T. A. Lin, T. Chatterjee, W. L. Tsai, W. K. Lee, M. J. Wu, M. Jiao, K. C. Pan, C. L. Yi, C. L. Chung, K. T. Wong, C. C. Wu, *Adv. Mater.*, 2016, **28**, 6976-6983.
12 G. Mehes, H. Nomura, Q. S. Zhang, T. Nakagawa, C. Adachi, *Angew. Chem. Int. Ed.*, 2012, **51**, 11311-11315.
13 Q. S. Zhang, J. Li, K. Shizu, S. P. Huang, S. Hirata, H. Miyazaki, C. Adachi, *J. Am. Chem. Soc.*, 2012, **134**, 14706-14709.
14 H. Kaji, H. Suzuki, T. Fukushima, K. Shizu, K. Suzuki, S. Kubo, T. Komino, H. Oiwa, F. Suzuki, A. Wakamiya, Y. Murata, C. Adachi, *Nat. Commun.*, 2015, **6**, 8476.
15 S. D. Xu, T. T. Liu, Y. X. Mu, Y. F. Wang, Z. G. Chi, C. C. Lo, S. W. Liu, Y. Zhang, A. Lien, J. R. Xu, *Angew. Chem. Int. Ed.*, 2015, **54**, 874-878.
16 K. Y. Sun, W. Jiang, X. X. Ban, B. Huang, Z. H. Zhang, M. Y. Ye, Y. M. Sun, *RSC Adv.*, 2016, **6**, 22137-22143.
17 R. Furue, T. Nishimoto, I. S. Park, J. Lee, T. Yasuda, *Angew. Chem. Int. Ed.*, 2016, **55**, 7171-7175.
18 K. Goushi, K. Yoshida, K. Sato, C. Adachi, *Nat. Photon.*, 2012, **6**, 234-248.
19 Y. S. Park, K. H. Kim, J. J. Kim, *Appl. Phys. Lett.*, 2013, **102**, 153306.
20 Z. Chen, X. K. Liu, C. J. Zheng, J. Ye, C. L. Liu, F. Li, X. M. Ou, C. S. Lee, X. H. Zhang, *Chem. Mater.*, 2015, **27**, 5206-5211.
21 D. Wang, W. L. Li, B. Chu, Z. S. Su, D. F. Bi, D. Y. Zhang, J. Z. Zhu, F. Yan, Y. R. Chen, T. Tsuboi, Appl. Phys. Lett. 2008, 92, 053304.
22 L. Song, Y. S. Hu, Z. Q. Liu, Y. Lv, X. Y. Guo, X. Y. Liu, *ACS Appl. Mater. Interface*, 2017, **9**, 2711-2719.
23 K. Goushi, C. Adachi, *Appl. Phys. Lett.*, 2012, **101**, 023306.
24 S. N. Bagriantsev, K. H. Ang, A. Gallardo-Godoy, K. A. Clark, M. R. Arkin, A. R. Renslo, D. L. Minor, *ACS Chem. Bio.*, 2013, **8**, 1841-1851.
25 M. C. Suh, S. R. Park, Y. R. Cho, D. H. Shin, P. G. Kang, D. A. Ahn, H. S. Kim, C. B. Kim, *ACS Appl. Mater. Interface*, 2016, **8**, 18256-18265.
26 B. Spingler, S. Schnidrig, T. Todorova, F. Wild, *CrystEngComm.*, 2012, **14**, 751-757.
27 H. Tanaka, K. Shizu, H. Nakanotani, C. Adachi, *J. Phys. Chem. C*, 2014, **118**, 15985-15994.
28 W. L. Tsai, M. H. Huang, W. K. Lee, Y. J. Hsu, K. C. Pan, Y. H. Huang, H. C. Ting, M. Sarma, Y. Y. Ho, H. C. Hu, C. C. Chen, M. T. Lee, K. T. Wong, C. C. Wu, *Chem. Commun.*, 2015, **51**, 13662-13665.
29 Y. N. Hong, J. W. Y. Lam, B. Z. Tang, *Chem. Soc. Rev.*, 2011, **40**, 5361-5388.
30 J. J. Guo, X. L. Li, H. Nie, W. W. Luo, S. F. Gan, S. M. Hu, R. R. Hu, A. J. Qin, Z. J. Zhao, S. J. Su, B. Tang, *Adv. Funct. Mater.*, 2017, **27**, 1606458.
31 H. Kuhn, *J. Chem. Phys.*, 1970, **53**, 101.
32 J. Lee, N. Aizawa, M. Numata, C. Adachi, T. Yasuda, *Adv. Mater.*, 2017, **29**, 1604856.

View Article Online
DOI: 10.1039/C8TC02590H

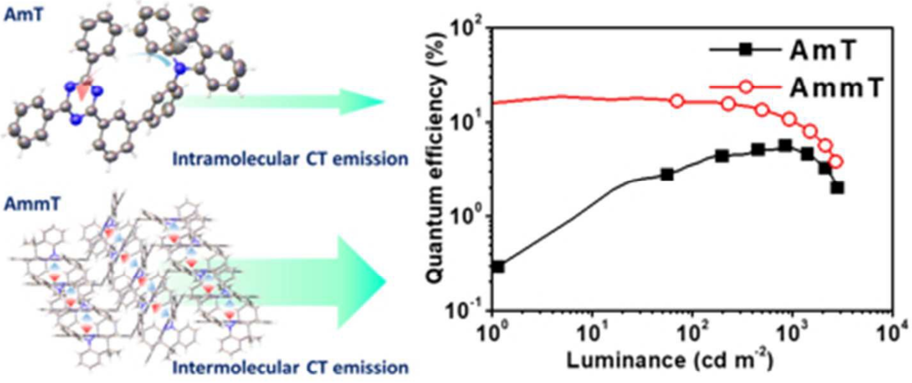

We report new TADF molecules (**AmT** and **AmmT**) for highly efficient non-doped OLEDs utilizing intra- and intermolecular charge transfer excitons.

80x40mm (150 x 150 DPI)